

# Density functional calculations of potential energy surface and charge transfer integrals in molecular triphenylene derivative HAT<sub>6</sub>

Mohamed Zbiri · Mark R. Johnson ·  
Gordon J. Kearley · Fokko M. Mulder

Received: 30 January 2009 / Accepted: 11 March 2009 / Published online: 1 April 2009  
© Springer-Verlag 2009

**Abstract** We investigate the effect of structural fluctuations on charge transfer integrals, overlap integrals, and site energies in a system of two stacked molecular 2,3,6,7,10,11-hexakis(hexyloxy)triphenylene (HAT<sub>6</sub>), which is a model system for conducting devices in organic photocell applications. A density functional based computational study is reported. Accurate potential energy surface calculations are carried out using an improved meta-hybrid density functional to determine the most stable configuration of the two weakly bound HAT<sub>6</sub> molecules. The equilibrium parameters in terms of the twist angle and co-facial separation are calculated. Adopting the fragment approach within the Kohn–Sham density functional framework, these parameters are combined to a lateral slide, to mimic structural/conformational fluctuations and variations in the columnar phase. The charge transfer and spatial overlap integrals, and site energies, which form the matrix element of the Kohn–Sham Hamiltonian are derived. It is found that these quantities are strongly affected by the conformational

variations. The spatial overlap between stacked molecules is found to be of considerable importance since charge transfer integrals obtained using the fragment approach differ significantly from those using the dimer approach.

**Keywords** Organic photocells · Columnar stacked HAT<sub>6</sub> · Density functional theory · Potential energy surface · Charge transfer integrals

## 1 Introduction

There has been growing interest in the use of organic materials for photovoltaic energy-conversion [1–5]. Due to their low cost, inherent flexibility and relative ease of processing, organic devices are a better alternative to the traditional, cost-prohibitive, inorganic semiconductors [6]. In this context, columnar discotic liquid-crystals [7] such as the triphenylene derivatives, hexakis(alkyloxy)triphenylenes (HAT<sub>n</sub>), are attractive model systems in the development of organic conducting devices [8]. Presently, our interest is focused on the 2,3,6,7,10,11-hexakis(hexyloxy)triphenylene system (HAT<sub>6</sub>) illustrated in Fig. 1. The HAT<sub>6</sub> molecule possesses a central planar aromatic core (mesogen) with peripheral chains that are attached to the disc-like core. The structural fluctuations are sufficient to suppress inhomogeneously distributed structural traps, instead, giving rise to a uniform “liquid-like” dynamic disorder [9] i.e. a liquid crystal composed of columns of molecules. The stacking between neighbouring disc-shaped molecules is due to the  $\pi$ – $\pi$  overlap originating from the delocalized  $\pi$ -orbitals above and below each aromatic core, and interactions between the aliphatic chains. This  $\pi$ – $\pi$  overlap provides a one-dimensional pathway for charge migration along the column direction [10]. However,

Dedicated to Professor Sandor Suhai on the occasion of his 65th birthday and published as part of the Suhai Festschrift Issue.

M. Zbiri · M. R. Johnson  
Laue Langevin Institute,  
38042 Grenoble Cedex 9, France

G. J. Kearley (✉)  
Bragg Institute, Australian Nuclear Science  
and Technology Organisation,  
Menai, NSW 2234, Australia  
e-mail: gke@ansto.gov.au

F. M. Mulder  
Department of Radiation,  
Radionuclides and Reactors,  
Delft University of Technology,  
2629 JB Delft, The Netherlands

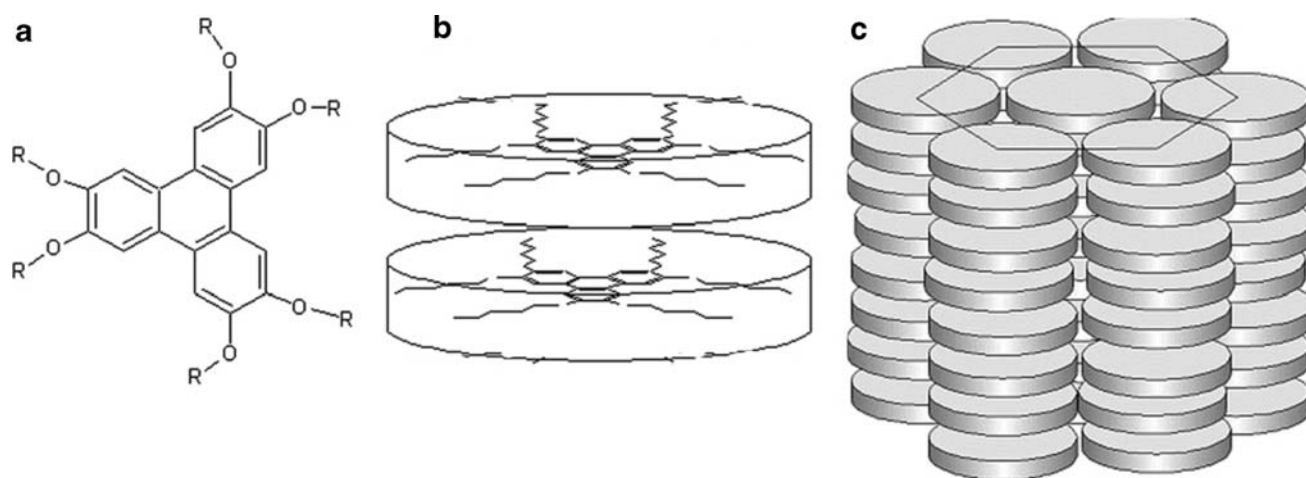


**Fig. 1** **a** Illustration of the HAT<sub>6</sub> molecule where  $R = C_6H_{13}$ . **b** Schematic illustration of a model system of two stacked molecules used in DFT calculations. **c** Hexagonal columnar arrangement in the discotic phase of HAT<sub>6</sub>

unlike inorganic devices, the spectral sensitivity of organic materials is limited. One of the major limitations is their narrow absorption window. Indeed, the diffusion length of excitons to the donor–acceptor interface is much shorter than the optical absorption length [11, 12]. Therefore, efficient energy conversion for practical applications requires significant improvements of charge transport and transfer processes [13–16]. In this context, a deeper understanding of the underlying structural mechanisms—which are responsible for the formation of the columnar phase—is of considerable importance. Previous studies of the HAT<sub>6</sub> have shown that structure and dynamics play a central role in the charge-transfer process of these materials. It was noted that the dynamics of the aromatic cores and the alkyl tails can affect the electronic properties [17–20].

We propose to go further in this study and to investigate computationally how charge transfer and hence charge carrier mobility are affected due to conformational fluctuations and structural disorder in the columnar liquid phase of HAT<sub>6</sub>. The HAT<sub>6</sub> molecule presents an aromatic core which is surrounded with six alkoxy tails that are required for columnar liquid crystal phase formation. A schematic representation is shown in Fig. 1a. The choice of the HAT<sub>6</sub> model system is justified by the optimum side-chain length that gives the broadest mesophase range. Between five and seven carbons in the alkyl tail are required for the columnar phase to form [18]. Further increase or decrease of the tail length reduces the temperature range of the hexagonal columnar (Col<sub>h</sub>) mesophase formation.

We have studied quantum chemically a model system which consists of two stacked HAT<sub>6</sub> molecules as illustrated in Fig. 1b. Since the fluctuations and disorder we aim to investigate suppress structural periodicity, periodic band structure simulations are not presently applicable. The

Kohn–Sham formulation of the DFT (KSDF) [21, 22] became a standard tool in modelling large molecular systems leading to results with increasing accuracy at a significantly lower computational cost compared to wavefunction methods. KSDF-based methods, which are adopted here in their standard or improved (hybrid and meta) forms, have allowed many quantum physical and chemical problems to be addressed with unprecedented efficiency. The present work, which is of fundamental nature, has three goals: (1) to determine the potential energy surface of the stacking HAT<sub>6</sub> molecules and extract the corresponding equilibrium parameters in terms of co-facial separation and twist angle between the stacked HAT<sub>6</sub> monomers, (2) to calculate charge transfer integrals (CTIs), overlap integrals, and site energies by modeling a defined structural disorder, and (3) to evaluate how these quantities vary upon the imposed conformational fluctuations.

This paper is organized as follows: in Sect. 2 the computational aspects of our calculations are reported. Section 3 is dedicated to the presentation of the results and discussion and finally, a summary of our main findings is provided in Sect. 4.

## 2 Computational details

The input HAT<sub>6</sub> geometry (144 atoms) was obtained by considering structures of benzene and hexyloxy for the aromatic core and tails ( $R = OC_6H_{13}$ ), respectively. A starting fully Planar  $D_{3h}$  symmetry was assumed, the only out-of plane atoms being the hydrogens of the tails.

Potential energy surface calculations were performed using the Gaussian program [23] (version 03–D01). The exchange–correlation (XC) meta-hybrid functional PBE1KCIS has been employed [24–28]. This functional,

which includes a defined amount of the exact Hartree–Fock exchange together with a high-level kinetic energy density, has been applied successfully for chemical problems involving weak interactions. PBE1KCIS is not available with standard route in Gaussian03. The keywords required in Gaussian03 to carry out the PBE1KCIS calculation are: #PBEKCIS IOp(3/76 = 0780002200) [28]. The 6-311++G\*\* Gaussian functions were adopted for all atomic types [29–31]. CTIs ( $J$ ), overlap integrals ( $S$ ) and site energies ( $\epsilon$ ) were derived using the fragment approach which is a unique feature of the Amsterdam density functional (ADF) package (release 2007.01) [32, 33]. ADF is also used to determine the molecular orbitals diagram (MO) for the HAT<sub>6</sub> molecule. The generalized gradient approximation (GGA) has been adopted. The exchange contribution to the GGA was approximated by the Becke gradient correction (Becke88) [34] and the correlation part by the Perdew–Wang correction (PW91c) [35–37]. A triple- $\zeta$  Slater type orbital (STO) basis set, plus one set of polarisation (TZP), was used [38]. The frozen core approximation was applied up to 1 s for carbon and oxygen atoms.

### 3 Results and discussion

#### 3.1 Single molecule calculations

The frontier MO diagram, depicted in Fig. 2, of a single HAT<sub>6</sub> molecule is first determined in order to confirm the expected delocalized  $\pi$ -character of the aromatic core. These MOs correspond to the followings irreducible representations under  $D_{3h}$  point group symmetry: HOMO-1 ( $A_1''$ ), HOMO ( $E''$ ), LUMO ( $E''$ ) and LUMO+1 ( $A_2''$ ). These levels have the following Kohn–Sham orbital energies: HOMO-1 (−5.127 eV), HOMO (−4.316 eV), LUMO (−1.167) and LUMO+1 (−1.160 eV). The HOMO–LUMO separation was  $\sim 3.2$  eV. Both are  $\pi$ -type MOs. The valence level orbital (HOMO) spreads over oxygens as well, which bridge the core and carbonic chains. This is of considerable importance since it shows that for a given geometrical configuration in the columnar liquid phase, the contribution on oxygens might change leading to a corresponding change of the  $C_{\text{core}}\text{--O}$  and  $\text{O--C}_{\text{tail}}$  bond order. Such changes could delocalize an excess of charge over the tails thereby conferring an electronic role on the tails, in addition to the mechanical role in stabilizing the mesoscopic columnar phase.

#### 3.2 Potential energy surface of two stacked molecules

Previous works which dealt with calculations of CTIs and related quantities in similar systems—using either the fragment approach or the dimer approach, or both

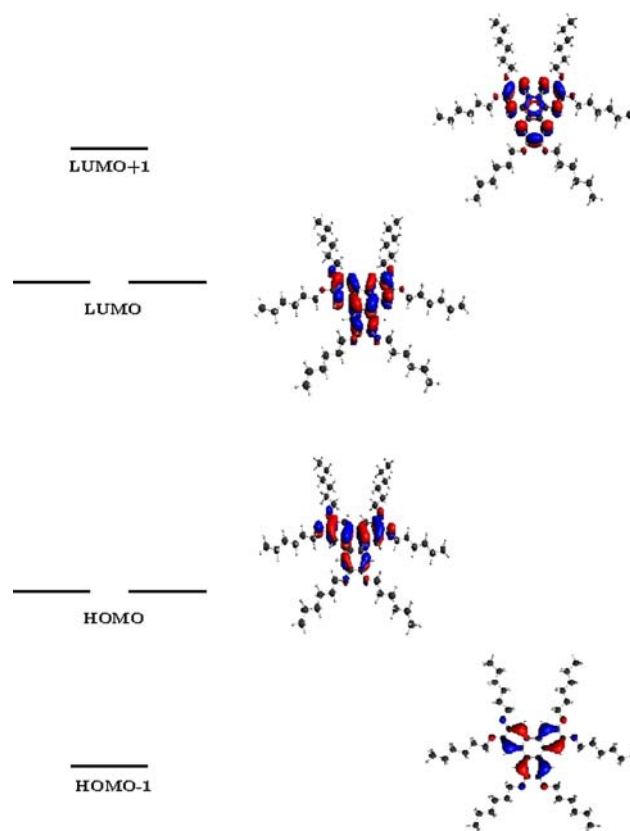


**Fig. 2** Frontier molecular orbital diagram for the HAT<sub>6</sub> molecule

(introduced hereafter)—used “probable” equilibrium structural parameters, justified qualitatively from van der Waals distances or from average experimental values [39–41].

Here, the starting point (equilibrium structure), before modeling structural fluctuations which are subsequently imposed on the HAT<sub>6</sub> stacked molecules, is the subject of careful investigation of the potential energy surface (PES). Three degrees of freedom can be modeled in practice at ab initio level to mimic structural fluctuations: the co-facial separation  $D$ , the twist angle  $\theta$  and the lateral slide or offset  $L$ . This is schematically illustrated in Fig. 4. We have calculated the PES of two stacked HAT<sub>6</sub> molecules using the accurately established DFT-based meta-hybrid functional PBE1KCIS. The latter has been recently applied successfully to weak interactions. Results are shown in Fig. 3. The 3-D PES highlights a clear energy minimum at  $\theta \sim 30^\circ$  and  $D \sim 3.5$  Å,  $L$  being kept fixed at 0 Å. This agrees well with previous works dedicated to similar systems with smaller aliphatic tails [40]. Other calculations (not reported here) were carried out using some standard semi-local, hybrid or meta functionals lead to a repulsive PES, i.e. no minima is found. The combination of hybrid and meta contributions in PBE1KCIS is presently adequate for treating weak interactions. For the sake of reliability, a

**Fig. 3** Left panel 3-D potential energy surface of the stacked HAT<sub>6</sub> molecules along the twist angle  $\theta$  and the co-facial separation  $D$ , with a zero offset ( $L = 0$  Å). Right panel cut along  $\theta$  with  $D = 3.5$  Å and  $L = 0$  Å

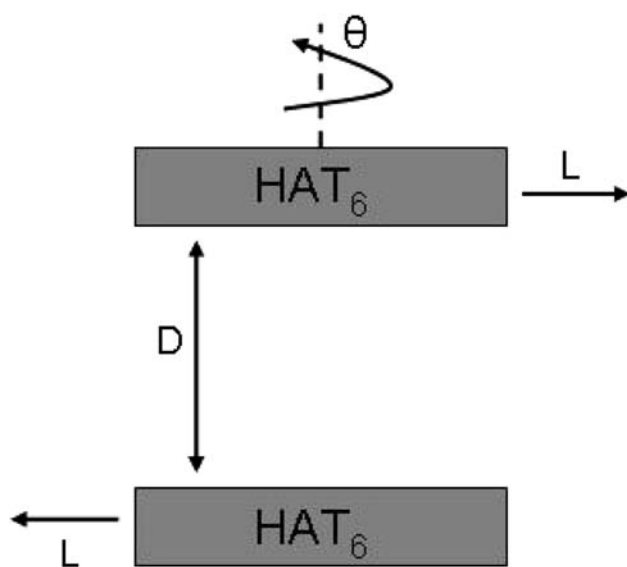
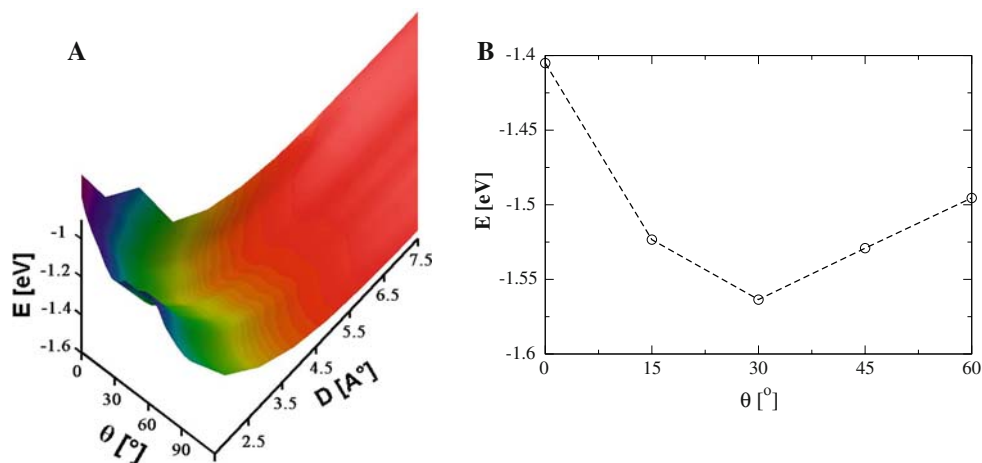


**Fig. 4** Schematic diagram of the modeled structural fluctuations between stacked HAT<sub>6</sub> molecules in the form of twist angle  $\theta$ , co-facial separation  $D$ , and lateral slide  $L$

detailed benchmark calculations done for several non-bonded systems are reported in references [28, 42, 43] (and references therein) in this regard. It is worth noting that DFT-based methods can nowadays be improved in an efficient way like wave function-based approaches. The systematic way to improve XC functionals has now been developed. In this context, ab initio DFT methods developed by Bartlett and coworkers are a good example [44].

### 3.3 Charge transfer integrals, overlap integrals and site energies

Having determined the equilibrium parameters of the stacked HAT<sub>6</sub> molecules, the next step is to use these parameters by varying them to mimic structural disorder

and to estimate how the HAT<sub>6</sub>–HAT<sub>6</sub> interaction is affected. This is done by evaluating CTIs, spatial overlap integrals  $S$ , and site energies. These quantities are a good indication on how conformational fluctuations in the columnar phase are important. We use the quantitative fragment orbital approach and a symmetry adapted linear combination of the HOMOs of the two HAT<sub>6</sub> molecules. The corresponding computational procedure is described in references [40, 41]. Briefly it can be summarized as follows: MOs are firstly calculated for each single HAT<sub>6</sub> forming the dimer in the specific orientation. Subsequently, MOs of the two stacked molecules are then expressed as a linear combination of the molecular orbitals of the monomer HAT<sub>6</sub> (fragment),  $\phi_i$ , leading to the overlap matrix  $S$ , the eigenvector matrix  $C$ , and the eigenvalue vector  $E$ . The relation  $\mathbf{h}_{KS} = \mathbf{SCEC}^{-1}$  provides the site energies,  $\langle \phi_i | \mathbf{h}_{KS} | \phi_i \rangle$ , and CTIs,  $\langle \phi_i | \mathbf{h}_{KS} | \phi_j \rangle$ . This procedure allows exact and direct calculations of  $J$ ,  $S$  and  $\epsilon$  as the diagonal and off-diagonal elements of the Kohn–Sham Hamiltonian  $\mathbf{h}_{KS}$ . For the sake of reliability, a second approach is adopted to estimate CTIs  $J$ . We will refer to it as the dimer approach. It is based on a zero spatial overlap assumption and can be used in some limited cases where the overlap between the interacting individual units forming a stacked system is negligible. The dimer approach consists of the use of the half energy splitting between the HOMO and HOMO-1 to get, qualitatively, the effective CTI.

Figure 5 presents the dependence of the charge transfer  $J$  on the twist angle  $\theta$  between two stacked HAT<sub>6</sub> molecules at a fixed distance  $D = 3.5$  Å as determined from PES calculations. Results of the fragment approach are compared to those obtained using the dimer approach. There is a significant difference between the methods due to the non-zero overlap neglected in the latter. Due to the  $D_{3h}$  point group symmetry, the angular dependence of  $J$  is periodic. The maximal and minimal values of  $J$  are 0.45 and 0.15 eV using the fragment approach, and 0.26

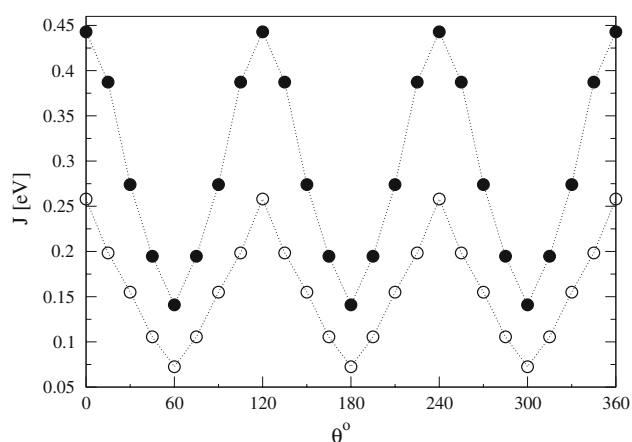


**Fig. 5** Calculated CTIs ( $J$ ) and their dependence on the twist angle  $\theta$  obtained using the fragment approach (*full circles*) and the dimer approach (*open circles*). The co-facial separation and the lateral slide between the two stacked HAT<sub>6</sub> molecules are kept fixed at  $D = 3.5 \text{ \AA}$  and  $L = 0 \text{ \AA}$ , respectively

**Table 1** Calculated site energies ( $\epsilon$ ) and spatial overlap integrals ( $S$ ) at  $D = 3.5 \text{ \AA}$  and  $L = 0.0 \text{ \AA}$ , using the fragment approach

$\theta$ ( $^\circ$ )	0	15	30	45	60
$\epsilon$ (eV)	-3.99	-4.01	-4.05	-4.07	-4.10
$S$	0.047	0.028 (2)	0.028 (1)	0.022	0.017

and 0.07 eV adopting the dimer approach. They correspond to twist angles  $n \times \frac{2\pi}{3}$  and  $\frac{\pi}{3} + n \times \frac{2\pi}{3}$ , respectively. Values of  $J$  increase periodically with the twist angle. When  $\theta \neq n\frac{\pi}{3}$ , there is a reduction in symmetry from  $D_{3h}$  to  $C_3$  point group, and if  $\theta = n\frac{\pi}{3}$  there is a reduction in symmetry from  $D_{3h}$  to  $C_{3v}$  occurs. Analogous to  $J$ , the spatial overlap, values gathered in Table 1, vary due to symmetry deviation from  $D_{3h}$ . The site energy  $\epsilon$  corresponding to the equilibrium parameters,  $\theta = 30^\circ$  and  $S = 3.5 \text{ \AA}$ , determined by PES calculations, is  $-4.05 \text{ eV}$ , see Table 1. Increasing the twist angle from  $0^\circ$  to  $60^\circ$  results in a change of  $\epsilon$  from  $-3.99$  to  $-4.10 \text{ eV}$  indicating that the interaction of individual HAT<sub>6</sub> molecules decreases, in agreement with the dependence of  $J$  and  $S$ . Figure 6 shows the exponential dependence of the charge transfer  $J$  on the co-facial separation  $D$  between two stacked HAT<sub>6</sub> molecules with a fixed twist angle  $\theta = 30^\circ$ , as determined from PES calculations. The point group symmetry is therefore  $C_3$ . Results derived using the fragment approach are compared to those obtained using the dimer approach. There is a significant difference between both methods due to the non-zero overlap neglected in the latter. The maximal and minimal values of  $J$  are 0.55 and 0.02 eV using the fragment approach, and 0.34 and 0.0 eV adopting the dimer approach. The value of  $J$  decreases exponentially with the separation  $D$ . The exponential decay parameter  $\beta$  is equal

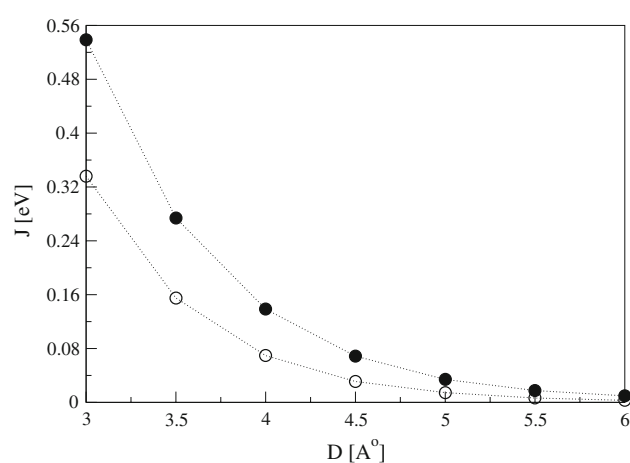


**Fig. 6** Calculated CTIs ( $J$ ) and their dependence on the co-facial separation  $D$  obtained using the fragment approach (*full circles*) and the dimer approach (*open circles*). The twist angle and the lateral slide between the two stacked HAT<sub>6</sub> molecules are kept fixed at  $\theta = 30^\circ$  and  $L = 0 \text{ \AA}$ , respectively

**Table 2** Calculated site energies ( $\epsilon$ ) and spatial overlap integrals ( $S$ ) at  $\theta = 30^\circ$  and  $L = 0.0 \text{ \AA}$ , using the fragment approach

$D$ ( $\text{\AA}$ )	3	3.5	4	4.5	5	5.5	6
$\epsilon$ (eV)	-4.05	-4.05	-4.06	-4.08	-4.10	-4.12	-4.14
$S$	0.050	0.028	0.016	0.009	0.005	0.003	0.002

to 1.4 and  $1.6 \text{ \AA}^{-1}$  for the fragment and dimer approaches, respectively. Analogous to  $J$ , the spatial overlap  $S$  values gathered in Table 2 decrease rapidly with increase of the co-facial separation  $D$  until reaching the long-range interaction limit at higher  $D$ , which is the monomeric zero overlap limit. Therefore, the charge transport description in terms of only the neighboring electronic couplings is adequate. Site energy  $\epsilon$  has the same value of  $-4.05 \text{ eV}$  at 3.0 and  $3.5 \text{ \AA}$  (see Table 2), the latter corresponding to the equilibrium distance. This indicates that repulsive effects are stabilized below  $D_0 = 3.5 \text{ \AA}$ . Increasing  $D$  to larger distances results in a change of  $\epsilon$  from  $-4.05$  to  $-4.14 \text{ eV}$ , indicating that the interaction of individual HAT<sub>6</sub> molecules decreases, in agreement with the dependence of  $J$  and  $S$ . It is worthwhile to investigate the lateral slide or offset  $L$  between the columnar stacked HAT<sub>6</sub> as a third degree of freedom which can perturb noticeably charge transfer processes through symmetry breaking, and hence spatial overlap. This is demonstrated in Fig. 7. Only results of the fragment approach are reported. The twist angle and co-facial separation were kept fixed at their equilibrium values, i.e.  $\theta_0 = 30^\circ$  and  $D_0 = 3.5 \text{ \AA}$ . The offset  $L$  is achieved by sliding one HAT<sub>6</sub> with respect to the other along a  $C_2$  axis. The maximal value of the charge transfer  $J$  is 0.27 eV. The complex nodal structure (nodes of the

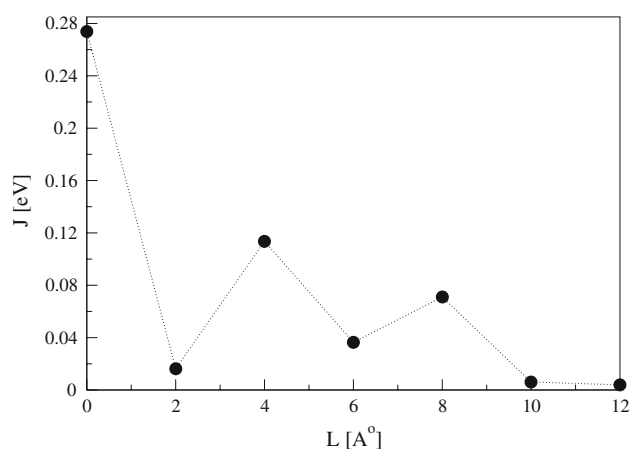


**Fig. 7** Calculated CTIs ( $J$ ) and their dependence on the lateral slide (offset)  $L$  between the two stacked HAT<sub>6</sub> molecules. The twist angle  $\theta$  and the co-facial separation  $D$  are kept fixed at their equilibrium values; 30° and 3.5 Å, respectively

**Table 3** Calculated site energies ( $\epsilon$ ) and spatial overlap integrals ( $S$ ) at  $\theta = 30^\circ$  and  $D = 3.5$  Å, using the fragment approach

$L$ (Å)	0	2	4	6	8	10
$\epsilon$ (eV)	-4.05	-4.11	-4.18	-4.29	-4.35	-4.37
$S$	0.0281	0.0151	0.0011	0.0008	0.0020	0.0004

wavefunction) which is perpendicular to the plane of the large HAT<sub>6</sub> molecule, is well reflected through local maxima and minima, which correspond to a constructive/destructive character of the overlap between the individual HAT<sub>6</sub> molecules. Spatial overlaps  $S$  show clearly such oscillations (see Table 3). A higher offset will result in a zero overlap, and hence zero charge transfer. At  $L = 0$  Å the site energy  $\epsilon$  is equal to  $-4.05$  eV, corresponding to the equilibrium parameters (see Table 3). When  $L$  increases, the site energy tends to the monomer limit  $-4.38$  eV, which will in this case be close to the eigenvalue of the HOMO of single HAT<sub>6</sub>.

#### 4 Summary

In summary we have determined, for the first time, the potential energy surface for a molecular model of two stacked HAT<sub>6</sub> molecules adopting an improved meta-hybrid density functional PBE1KCIS, which is well suited for weak molecular interactions [28]. Clear minima have been found corresponding to a twist angle  $\theta$  and co-facial separation  $D$  of  $\sim 30^\circ$  and  $\sim 3.5$  Å, respectively. The dimer equilibrium geometry was determined with the constraint  $L = 0$  Å.

Charge transfer integrals, overlap integrals and site energies relevant to charge transport in columnar HAT<sub>n</sub> have been evaluated using the unique molecular fragment approach as implemented in the ADF software [32, 33]. The importance of the spatial overlap between stacked molecules is highlighted by comparing CTIs obtained from the fragment approach to those calculated from the half energy splitting between the HOMO and HOMO-1 in the dimer. A significant difference is found due to the non-zero overlap integral in the former. CTIs vary strongly as a function of the intermolecular packing geometry. The angle dependence is periodic and the distance (co-facial separation) dependence is exponential. At larger distances, the monomer limit is reached and there is no charge transfer. Effect of the offset between the two columnar stacked HAT<sub>6</sub> molecules reveals the destructive/constructive character and the complex nodal structure of the wave function of the large HAT<sub>6</sub> system. The work presented in this paper extends work by other authors [40] on HAT<sub>1</sub> and comparable molecules. The molecule studied here, HAT<sub>6</sub>, is almost three times bigger than the molecules studied previously. By using a meta-hybrid functional, we have determined the equilibrium geometry of a pair of HAT<sub>6</sub> molecules, whereas this initial geometry was inferred in previous work. Results concerning charge transfer and overlap integrals and site energies are qualitatively similar to those obtained for HAT<sub>1</sub>. Long molecular tails are essential in stabilizing the columnar, conducting liquid crystal phase. Normal mode calculations in ground and excited electronic states also suggest that the structure and vibrations of the molecular tails are sensitive to the molecular electronic structure [45]. Practically, in the presence of dynamic and/or static structural fluctuations the mobility, and therefore the conductivity, should scale approximately quadratically with the charge transfer integral as it has been reported for similar organic materials [40, 46, 47]. Thus, the data reported here can be used to estimate quantitatively charge transport properties in tri-phenylene derivatives. Following the work presented in this paper, we are in a position to extend this level of analysis to more realistic structural fluctuations, obtained from molecular dynamics simulations of the liquid crystal. Our aim is to establish the mechanical and electronic role of the molecular tails in HAT-based materials.

#### References

- Schmidt-Mende L, Fechtenkötter A, Müllen K, Moons E, Friend RH, MacKenzie JD (2001) *Science* 293:1119
- Forrest SR (2005) *Nature (Lond)* 87:233508
- Xue J, Uchida S, Rand BP, Forrest SR (2004) *App Phys Lett* 85:5757

4. Yu, G, Gao J, Hummelen JC, Wudl F, Heeger AJ (1995) *Science* 270:1789
5. Peumans P, Uchida S, Forrest SR (2003) *Nature* 425:158
6. Xue J, Uchida S, Rand BP, Forrest SR (2004) *App Phys Lett* 84:3013
7. Chandrasekhar S, Raganath GS (1990) *Rep Prog Phys* 53:57
8. Boden N, Bissel R, Clements J, Movaghar B (1996) *Curr Sci* 71:599
9. Shen X, Dong RY, Boden N, Bushby RJ, Martin PS, Wood A (1998) *J Chem Phys* 108:4324
10. Adam D, Schumacher B, Simmere J, Etbach KH, Ringsdorf H, Haarer D (1994) *Nature (Lond)* 371:142
11. Xue J, Uchida S, Rand B, Forrest S (2004) *Appl Phys Lett* 85:5757
12. Yang F, Lunt R, Forrest S (2008) *Appl Phys Lett* 92:053310
13. Dreschel J, Mannig B, Kozlowski F, Pfeiffer M, Leo K, Hope H (2005) *App Phys Lett* 86:244102
14. Cheyins D, Gommans H, Odijk M, Poortmans J, Heremans P (2007) *Sol Ener Mat* 91:399
15. Rand BP, Xue J, Yang F, Forrest SR (2005) *App Phys Lett* 87:233508
16. Soci C, Moses D, Xu QH, Heeger AJ (2005) *Phys Rev B* 72:245204
17. Mulder FM, Stride J, Picken SJ, Kouwer PHJ, de Haas MP, Siebbeles LDA, Kearley GJ (2003) *J Am Chem Soc* 125:3860
18. Kruglova O, Mulder FM, Siebbeles LDA, Kearley GJ (2006) *Chem Phys* 330:333
19. Kruglova O, Mulder FM, Kotlewski A, Picken SJ, Parker S, Johnson MR, Kearley GJ (2006) *Chem Phys* 330:360
20. Kearley GJ, Mulder FM, Picken SJ, Kouwer PHJ, Stride J (2003) *Chem Phys* 292:185
21. Hohenberg P, Kohn W (1964) *Phys Rev* 136:B864–B871
22. Kohn W, Sham L (1965) *Phys Rev* 140:A1133
23. Frisch MJ, Trucks GW, Schlegel HB, Scuseria GE, Robb MA, Cheeseman JR, Montgomery JA Jr, Vreven T, Kudin KN, Burant JC, Millam JM, Iyengar SS, Tomasi J, Barone V, Mennucci B, Cossi M, Scalmani G, Rega N, Petersson GA, Nakatsuji H, Hada M, Ehara M, Toyota K, Fukuda R, Hasegawa J, Ishida M, Nakajima T, Honda Y, Kitao O, Nakai H, Klene M, Li X, Knox JE, Hratchian HP, Cross JB, Bakken V, Adamo C, Jaramillo J, Gomperts R, Stratmann RE, Yazyev O, Austin AJ, Cammi R, Pomelli C, Ochterski JW, Ayala PY, Morokuma K, Voth GA, Salvador P, Dannenberg JJ, Zakrzewski VG, Dapprich S, Daniels AD, Strain MC, Farkas O, Malick DK, Rabuck AD, Raghavachari K, Foresman JB, Ortiz JV, Cui Q, Baboul AG, Clifford S, Cioslowski J, Stefanov BB, Liu G, Liashenko A, Piskorz P, Komaromi I, Martin RL, Fox DJ, Keith T, Al-Laham MA, Peng CY, Nanayakkara A, Challacombe M, Gill PMW, Johnson B, Chen W, Wong MW, Gonzalez C, Pople JA (2004) *Gaussian 03*, revision d.01. Gaussian, Inc., Wallingford
24. Perdew JP, Burke K, Ernzerhof M (1996) *Phys Rev Lett* 77:3865
25. Rey J, Savin A (1998) *Int J Quantum Chem* 69:581
26. Krieger JB, Chen J, Iafate GJ, Savin A (1996) In: Gonis A, Kioussis N (eds) *Electron correlations and materials properties*. Plenum, New York, p 463
27. Toulouse J, Savin A, Adamo C (2002) *J Chem Phys* 117:10465
28. Zhao Y, Truhlar DG (2005) *J Chem Theory Comput* 1:415
29. Rassolov VA, Ratner MA, Pople JA, Redfern PC, Curtiss LA (2001) *J Comput Chem* 22:976
30. Petersson GA, Al-Laham MA (1991) *J Chem Phys* 94:6081
31. Raghavachari K, Trucks GW (1989) *J Chem Phys* 91:1062
32. ADF, Amsterdam density functional program (2006) *Theoretical chemistry*. Vrije Universiteit, Amsterdam. <http://www.scm.com>
33. te Velde G, Bickelhaupt FM, Baerends EJ, Guerra CF, van Gisbergen SJA, Snijders JG, Ziegler T (2001) *J Comput Chem* 22:931
34. Becke A (1988) *Phys Rev A* 38:3098
35. Perdew J (1986) *Phys Rev B* 33:8822
36. Perdew J (1986) *Phys Rev B* 34:7406
37. Perdew J, Chevary J, Vosko S, Jackson K, Pederson M, Singh D, Fiolhais C (1992) *Phys Rev B* 46:6671
38. Lenthe EV, Baerends EJ (2003) *J Comput Chem* 24:1142
39. Huang J, Kertesz M (2005) *J Chem Phys* 122:234707
40. Senthilkumar K, Grozema FC, Bickelhaupt FM, Siebbeles LDA (2003) *J Chem Phys* 119:9809
41. Santhanamoorthi N, Kolandaivel P, Senthilkumar K (2006) *J Phys Chem A* 110:11551
42. Wang H-J, Fu Y (2009) *J Mol Struct (Theochem)* 893:67
43. Riley KE, Op't Holt BT, Merz KM (2007) *J Chem Theory Comput* 3:407
44. Bartlett RJ, Lotrich VF, Schweigert IV (2005) *J Chem Phys* 123:062205
45. Zbiri M, Johnson MR, Kearley GJ, Mulder FM (2009) (in press)
46. Wegewijs BR, Siebbeles LDA, Boden N, Bushby RJ, Movaghar B, Lozman OR, Liu Q, Pecchia A, Mason LA (2002) *Phys Rev B* 65:245112
47. Palenberg MA, Silbey RJ, Malagoli M, Bredas JL (2000) *J Chem Phys* 112:1541
48. Vosko SH, Wilk L, Nusair M (1980) *Can J Chem* 58:1200